Acta Cryst. (1963). **16**, 282

Dynamical Diffraction Theory of Waves in Distorted Crystals. II. Perturbation Theory

BY N. KATO

H. H. Wills Physics Laboratory, University of Bristol, England and Department of Applied Physics, Nagoya University, Nagoya, Japan

(*Received* 10 *August* 1961 *and in revised form* 7 *March* 1962)

As a special application of the 'lamellar-crystal theory' described in Part I, a two-wave theory is developed for distorted crystals in which the individual lamellae are perfect in lateral directions. A perturbation approach is used in practical applications so that slightly distorted crystals are mainly concerned. An apparent departure from Friedel's law on (h, k, l)- and $(\bar{h}, \bar{k}, \bar{l})$-reflections in X-ray topographs (Lang, private communication) is interpreted as an effect of a slight lattice-bending in the presence of the Borrmann absorption. The distortion of Pendellösung fringes due to a lattice bending in electron cases as well as in X-ray cases is also explained. The applicability of the present two-wave theory to crystals having an arbitrary distortion is discussed together with the justification for the column approximation (Hirsch *et al.*, 1960).

1. Introduction

Most of diffraction theories applied to distorted crystals are formulated on the base of the wave-kinematical approximation since they are mainly concerned with highly distorted regions in small crystallites (Warren & Averbach, 1950; Wilson, 1952). Recent direct observations of lattice defects in a single crystal by means of electrons (Hirsch *et al.*, 1956) as well as by X-rays (Lang, 1958; Borrmann *et al.*, 1958; Newkirk, 1958) have stimulated the development of the wave-dynamical theory applicable to distorted crystals.

So far a few attempts along this line have been reported in electron problems.* Heidenreich (1949) has dealt with a homogeneously bending crystal and Hashimoto *et al.* (1960) have been concerned with an edge dislocation lying in a crystal parallel to the incident wave. The principal idea used by them is to divide a distorted crystal into many parts or columns† along the direction of the incident wave and to apply a perfect-crystal theory to an individual column. The essential assumption is that the lattice is perfect within these columns in any sense. Thus their theories may be called 'perfect-crystal column theories'.

In the present paper, it will be shown that the two-wave theory of Part I (Kato, 1963) can be developed for the case of distorted crystals in which distortion occurs along a direction of wave propagation. Fundamental aspects of the theory will be described in § 2. In order to obtain practical results we use a perturbation approximation. In § 3 and § 4 the following two experiments are explained respectively in terms of the present theory; (*a*) an apparent departure from the Friedel law on (h, k, l) and $(\bar{h}, \bar{k}, \bar{l})$ reflections in X-ray topographs (Lang, private communication) and (*b*) the bending of Pendellösung fringes due to lattice distortion in electron cases as well as in X-ray cases.

Since the present theory is a 'two-wave theory', we must necessarily assume that the crystal slices are perfect in lateral directions but displaced relative to one another If, however, we combine the present theory with the column approximation we may apply the theory to more general cases of lattice distortions. So far the column approximation is not used with any sufficient justification particularly in a wave-dynamical sense, although the approximation itself is very fundamental for the theory of Heidenreich and Hashimoto *et al.*, as well as for the present one. In § 5, using the diaphragm consideration (Kato, 1952), two semi-quantitative criterions are given for justifying the column approximation.

2. Two-wave theory for distorted crystals

Any deformation of lattice can be described in terms of the displacement of lattice points as a function of positions in the undeformed state. If the local variation of the displacement is small enough, lattice conception is retained. Then we can define also reciprocal lattice vectors as a function of positions in real space. In this paper we are concerned with only such small distortions.

(*a*) *Two-wave theory*

In this section we consider cases in which the

* The author was informed during the preparation of this work that Howie & Whelan were developing independently a theory which was equivalent to the present theory in fundamental points. Their paper has been published already (1961). (Note added in the revision.)

† The word 'columns' was used first by Hirsch *et al.* (1960) in their kinematical theory on dislocation images in electron-micrographs.

lattice is *perfect and homogeneous in lateral directions.* Here lateral implies parallel to the incident surface of the crystal. Thus any dilatation, tilting or rotation is not allowed for the upper part of the crystal with respect to the lower part. Otherwise some misfits between upper and lower parts of the crystal may occur and violate the homogeneity of the lattice in lateral directions. Under this limitation the whole crystal can be divided into crystal slices by perfect lattice planes which are equivalent and parallel to the incident surface. Thus the diffraction phenomena in an individual crystal slice can be treated in the same way as shown in Part I for perfect crystals. Next we consider a net plane which is inclined with respect to the incident surface. In perfect crystals the net plane should be perfectly plane. Now this restrictive condition is taken off. In the distorted crystals with which we are concerned here the inclined lattice planes are allowed to be bent with going into the crystal. The lattice distortion of this type is specified only by giving the displacements of the crystal slices (or of equivalent axes).

We take x_n- and y_n-axes and their corresponding reciprocal axes on the top surface of each slice with the origins placed at the equivalent lattice points. With respect to these coordinate axes we can define the following notations as in Part I.

$\{p_n, q_n\}$: The relative displacements of nth crystal-slice with respect to $(n-1)$th slice in lateral directions.

Δz_n: The thickness of the crystal slice.

(ξ, η, ζ): The components of the wave vector of the incident wave in the reciprocal space.

(ξ', η', ζ'): The components of the wave vector of the diffracted wave in the reciprocal space.

(g_1, g_2, g_3^n): The components of the reciprocal lattice vector $\mathfrak{g}^n$ of the net plane* with which we are concerned.

Since the lattice is assumed as perfect in lateral directions g_1 and g_2 are constant throughout the crystal whereas g_3^n may not be so. Among these quantities the relation

$$g_1 p_n + g_2 q_n + g_3^n \Delta z_n = 0 \tag{1}$$

should be held, since the vector $\mathfrak{g}^n$ is perpendicular to the net plane concerned.

The components (ξ, η) and (ξ', η') are connected with each other by

$$(\xi', \eta') = (\xi, \eta) + 2\pi(g_1, g_2) . \tag{2}$$

In addition ζ and ζ' are directly given by (ξ, η) and (ξ', η') respectively because the magnitude of the wave vectors is always K. Consequently the components (ξ, η, ζ) and (ξ', η', ζ') are constant throughout the crystal. Thus only two waves are sufficient to account for the crystal waves.

Finally a parameter is defined by

$$\varphi_n = \tfrac{1}{2}(\zeta - \zeta' - 2\pi g_3^n) \tag{3}$$

for each slice. This indicates the departure of the incident wave from the exact Bragg condition.

Using these relations we can obtain the relation between the Fourier transforms of the wave function, $\mathbf{F}_n$ and $\mathbf{F}_{n+1}$ for the nth and $(n+1)$th slices (*cf.* equation (I·33)),

$$\mathbf{F}_{n+1} = (\mathbf{d}_n \zeta_n \mathbf{Q}_n)\mathbf{F}_n . \tag{4}$$

Here ζ_n, $\mathbf{Q}_n$ and $\mathbf{d}_n$ are given by equations (I·30), (I·31) and (I·32) respectively. Like the cases of perfect crystals we can make the matrix product symmetrical as

$$\mathbf{d}_n \zeta_n \mathbf{Q}_n = \exp i\Phi_n . \mathbf{R}_n \tag{5}$$

where Φ_n and $\mathbf{R}_n$ are given by

$$\Phi_n = (\xi p_n + \eta q_n + \zeta \Delta z_n) + \tfrac{1}{2}(\Phi_t + \Phi_r)\Delta z_n - \varphi_n \Delta z_n \tag{6}$$

$$\mathbf{R}_n = \begin{pmatrix} \exp i\varphi_n \Delta z_n & 0 \\ 0 & \exp -i\varphi_n \Delta z_n \end{pmatrix} \begin{pmatrix} a & ib_{12}\Delta z_n \\ ib_{21}\Delta z_n & a^* \end{pmatrix} . \tag{7}$$

They are the generalized equations of equations (I·38) and (I·39) respectively. Notations φ_t, φ_r, a, b_{12} and b_{21} have the same meanings as those in Part I. Thus the problem is reduced to calculation of the matrix product

$$\mathbf{K}_N = \mathbf{R}_N \mathbf{R}_{N-1} \ldots \mathbf{R}_1 . \tag{8}$$

Similarly to equation (I·41) we diagonalize a matrix

$$\mathbf{R}_n = \mathbf{X}_n \begin{pmatrix} \exp \lambda_{11}^n & 0 \\ 0 & \exp \lambda_{22}^n \end{pmatrix} \mathbf{X}_n^{-1} \tag{9}$$

$$= \mathbf{X}_n \boldsymbol{\lambda}_n \mathbf{X}_n^{-1} \tag{9'}$$

where $\mathbf{X}_n$ and $\mathbf{X}_n^{-1}$ are the right and the left eigenmatrix of $\mathbf{R}_n$, respectively, and $\exp \lambda_{ii}^n$ are the eigenvalues. The latter are given by equation (I·42) for each slice.

Thus

$$\begin{aligned} \lambda_{11}^n &= i(\varphi_n^2 + B^2)^{\frac{1}{2}} \Delta z_n \\ \lambda_{22}^n &= -i(\varphi_n^2 + B^2)^{\frac{1}{2}} \Delta z_n \end{aligned} \tag{10}$$

where φ_n stands for the parameter φ_D of the nth slice.

With this notation

$$\mathbf{K}_N = \mathbf{X}_N \mathbf{H}_N \mathbf{X}_N^{-1} \tag{11}$$

where

$$\mathbf{H}_N = \boldsymbol{\lambda}_N \mathbf{E}_{N-1} \boldsymbol{\lambda}_{N-1} \ldots \mathbf{E}_1 \boldsymbol{\lambda}_1 \tag{12}$$

and

$$\mathbf{E}_n = \mathbf{X}_{n+1}^{-1} \mathbf{X}_n . \tag{13}$$

In the present problem difficulties arise in that $\mathbf{E}_n$ is no longer a unit matrix. It may be expected, however, that $\mathbf{E}_n$ is close to a unit matrix if distortions are sufficiently small. In fact, writing

* Strictly speaking, this should be called 'net surface' since it can be defined as a plane only in a localized region. Since no ambiguity is expected 'net plane' will be used hereafter.

$$\mathbf{E}_n=\begin{pmatrix}1+\varepsilon_{11}^n & \varepsilon_{12}^n\\ \varepsilon_{21}^n & 1+\varepsilon_{22}^n\end{pmatrix}\simeq\begin{pmatrix}\exp\varepsilon_{11}^n & \varepsilon_{12}^n\\ \varepsilon_{21}^n & \exp\varepsilon_{22}^n\end{pmatrix} \quad (14)$$

we have, for example,

$$\varepsilon_{11}^n=\{[\varphi_n+(\varphi_n^2+B^2)^{\frac{1}{2}}]/(\varphi_n^2+B^2)^{\frac{1}{2}}\}\Delta z_n(\Delta\varphi_n/2)i + \{[\varphi_n-(\varphi_n^2+B^2)^{\frac{1}{2}}]/(\varphi_n^2+B^2)\}(\Delta\varphi_n/2)$$

where

$$\Delta\varphi_n=\varphi_{n+1}-\varphi_n\,.$$

In the expression for ε_{11}^n the imaginary part decreases with decreasing thickness Δz_n and the factor $\Delta\varphi_n$ is of an order of magnitude $\Delta z_n\simeq 10^{-8}$ cm. On the other hand the real part is independent of Δz_n and the factor $\Delta\varphi_n$ is of an order B^{-1}, namely larger than 10^{-4} cm. in X-ray cases and 10^{-6} cm. in electron cases. So we can safely neglect the imaginary part. Thus we have finally

$$\begin{aligned}\varepsilon_{11}^n&\simeq\frac{\varphi_n-(\varphi_n^2+B^2)^{\frac{1}{2}}}{\varphi_n^2+B^2}\left(\frac{\Delta\varphi_n}{2}\right)\\ \varepsilon_{22}^n&\simeq\frac{\varphi_n+(\varphi_n^2+B^2)^{\frac{1}{2}}}{\varphi_n^2+B^2}\left(\frac{\Delta\varphi_n}{2}\right)\\ \varepsilon_{12}^n&\simeq\frac{-\varphi_n+(\varphi_n^2+B^2)^{\frac{1}{2}}}{\varphi_n^2+B^2}\left(\frac{\Delta\varphi_n}{2}\right)\\ \varepsilon_{21}^n&\simeq\frac{-\varphi_n-(\varphi_n^2+B^2)^{\frac{1}{2}}}{\varphi_n^2+B^2}\left(\frac{\Delta\varphi_n}{2}\right)\end{aligned} \quad (15)$$

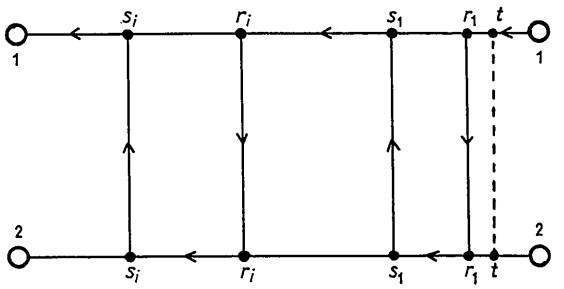

Fig. 1. Schematic diagram of matrix calculation. Bridging t–t should be inserted for calculating odd-order matrix $H_{ij}^{(2n+1)}$.

The magnitude of these quantities is of an order $(\Delta\varphi_n/B)$ at most. The quantity $\Delta\varphi_n$ is the change of φ_n due to the bending of the net plane concerned between the neighbouring slices. In perfect crystals the Bragg condition is satisfied at $\varphi_D=0$ and by increasing φ_D by the amount of B the diffracted intensity decreases to the half of the maximum value at the Bragg condition. Thus, neglecting a numerical factor, $\Delta\varphi_n/B$ is a ratio of a bending angle of the net plane per one slice and the angular width of the Bragg reflection.

If $\{\varepsilon_{ij}\}$'s are small enough compared with 1, we can expand the matrix $\mathbf{H}_N$ in the power series:

$$\mathbf{H}_N=\begin{pmatrix}H_{11}^{(0)} & 0\\ 0 & H_{22}^{(0)}\end{pmatrix}+\begin{pmatrix}0 & H_{12}^{(1)}\\ H_{21}^{(1)} & 0\end{pmatrix}+\begin{pmatrix}H_{11}^{(2)} & 0\\ 0 & H_{22}^{(2)}\end{pmatrix}+\cdots. \quad (16)$$

The matrix elements in this expression are calculated in terms of $\{\lambda_{ij}^n\}$ and $\{\varepsilon_{ij}^n\}$ considering a topological diagram shown in Fig. 1. Segments on the line 1–1 and 2–2 correspond to a multiplication through diagonal elements of $\mathbf{E}_n$ in equation (12). Bridging elements such as s_i–s_i and r_i–r_i correspond to multiplication through skew elements of $\mathbf{E}_n$ by which a switching is operated from multiplication of $\exp\{\varepsilon_{11}^n\lambda_{11}^n\}$ to multiplication of $\exp\{\varepsilon_{22}^n\lambda_{22}^n\}$ or *vice versa*. The suffixes s_i and r_i specify the switching matrices. Matrix elements of $\mathbf{H}_N$ are the sum of products corresponding to all possible routes from the right j-terminal to the left i-terminal. The expansion of equation (16) implies a classification of these routes in terms of the number of bridgings. Following this consideration we have

$$\left.\begin{aligned}H_{11}^{(0)}&=\exp\sum_{i=1}^{N}(\varepsilon_{11}^i+\lambda_{11}^i)\\ H_{22}^{(0)}&=\exp\sum_{i=1}^{N}(\varepsilon_{22}^i+\lambda_{22}^i)\end{aligned}\right\} \quad (17)$$

$$\left.\begin{aligned}H_{12}^{(1)}&=H_{11}^{(0)}\sum_{n=1}^{N}\varepsilon_{12}^n\exp\sum_{i=1}^{n}(\varepsilon_{22}^i+\lambda_{22}^i-\varepsilon_{11}^i-\lambda_{11}^i)\\ H_{21}^{(1)}&=H_{22}^{(0)}\sum_{n=1}^{N}\varepsilon_{21}^n\exp\sum_{i=1}^{n}(\varepsilon_{11}^i+\lambda_{11}^i-\varepsilon_{22}^i-\lambda_{22}^i)\,.\end{aligned}\right\} \quad (18)$$

Changing the summation to an integral it follows from equation (10) that

$$\left.\begin{aligned}\sum_{i=1}^{n}\lambda_{11}^i&=i\int_0^z(\varphi^2+B^2)^{\frac{1}{2}}dz\\ \sum_{i=1}^{n}\lambda_{22}^i&=-i\int_0^z(\varphi^2+B^2)^{\frac{1}{2}}dz\,,\end{aligned}\right\} \quad (19)$$

where φ is used in the place of φ_n and assumed as a continuous function of z.

Moreover from equation (15)

$$\begin{aligned}\sum_{i=1}^{n}\varepsilon_{11}^i&=\log\left(\frac{\alpha_n}{\alpha_1}\right)-\log\left(\frac{\beta_n}{\beta_1}\right)\\ \sum_{i=1}^{n}\varepsilon_{22}^i&=\log\left(\frac{\alpha_n}{\alpha_1}\right)-\log\left(\frac{\gamma_n}{\gamma_1}\right)\\ \sum_{i=1}^{n}\varepsilon_{12}^i&=\log\left(\frac{\alpha_1}{\alpha_n}\right)+\log\left(\frac{\beta_n}{\beta_1}\right)\\ \sum_{i=1}^{n}\varepsilon_{21}^i&=\log\left(\frac{\alpha_1}{\alpha_n}\right)+\log\left(\frac{\gamma_n}{\gamma_1}\right),\end{aligned} \quad (20)$$

where

$$\alpha_n=(\varphi_n^2+B^2)^{\frac{1}{2}}$$

$$\beta_n=\{\varphi_n+(\varphi_n^2+B^2)^{\frac{1}{2}}\}^{\frac{1}{2}} \quad (21)$$

$$\gamma_n=\{\varphi_n-(\varphi_n^2+B^2)^{\frac{1}{2}}\}^{\frac{1}{2}}. \quad (22)$$

Here we can see

$$\beta_n\gamma_n=iB\,. \quad (23)$$

By inserting these into equations (17) and (18), the matrix elements of $\mathbf{H}_n$ are given as follows:

$$H_{11}^{(2n)}=\left(\frac{\alpha_N}{\alpha_1}\right)\left(\frac{\beta_1}{\beta_N}\right)I_{11}^{(2n)}\exp i\int_0^z(\varphi^2+B^2)^{\frac{1}{2}}dz$$

$$H_{22}^{(2n)}=\left(\frac{\alpha_N}{\alpha_1}\right)\left(\frac{\gamma_1}{\gamma_N}\right)I_{22}^{(2n)}\exp -i\int_0^z(\varphi^2+B^2)^{\frac{1}{2}}dz \quad (24)$$

$$H_{12}^{(2n+1)}=\left(\frac{\alpha_N}{\alpha_1}\right)(\beta_1\beta_N)^{-1}I_{12}^{(2n+1)}\exp i\int_0^z(\varphi^2+B^2)^{\frac{1}{2}}dz$$

$$H_{21}^{(2n+1)}=\left(\frac{\alpha_N}{\alpha_1}\right)(\gamma_1\gamma_N)^{-1}I_{21}^{(2n+1)}\exp -i\int_0^z(\varphi^2+B^2)^{\frac{1}{2}}dz, \quad (25)$$

where

$$I_{11}^{(0)}=I_{22}^{(0)}=1 \quad (26)$$

and

$$I_{12}^{(1)}=\frac{B^2}{2}\int_{\varphi_1}^{\varphi_N}\frac{d\varphi}{\varphi^2+B^2}\exp -2i\int_0^z(\varphi^2+B^2)^{\frac{1}{2}}dz$$

$$I_{21}^{(1)}=\frac{B^2}{2}\int_{\varphi_1}^{\varphi_N}\frac{d\varphi}{\varphi^2+B^2}\exp 2i\int_0^z(\varphi^2+B^2)^{\frac{1}{2}}dz\,. \quad (27)$$

General terms $I_{ii}^{(2n)}$ and $I_{ij}^{(2n+1)}$ are given in the Appendix.

Once we have the matrix elements of $\mathbf{H}_N$, we can write down $\mathbf{K}_N$-matrix from equation (11) as follows:

$$K_{11}=\frac{1}{2\alpha_1\alpha_N}\left[A_+\exp i\int_0^z(\varphi^2+B^2)^{\frac{1}{2}}dz - A_-.\exp -i\int_0^z(\varphi^2+B^2)^{\frac{1}{2}}dz\right]$$

$$K_{22}=\frac{1}{2\alpha_1\alpha_N}\left[-B_+\exp i\int_0^z(\varphi^2+B^2)^{\frac{1}{2}}dz + B_-.\exp -i\int_0^z(\varphi^2+B^2)^{\frac{1}{2}}dz\right] \quad (28)$$

$$K_{12}=\frac{b_{12}}{2\alpha_1\alpha_N}\left[C_+\exp i\int_0^z(\varphi^2+B^2)^{\frac{1}{2}}dz - C_-.\exp -i\int_0^z(\varphi^2+B^2)^{\frac{1}{2}}dz\right]$$

$$K_{21}=\frac{b_{21}}{2\alpha_1\alpha_N}\left[D_+\exp i\int_0^z(\varphi^2+B^2)^{\frac{1}{2}}dz - D_-.\exp -i\int_0^z(\varphi^2+B^2)^{\frac{1}{2}}dz\right] \quad (29)$$

where

$$A_+=\beta_N^2D_+=\beta_1\beta_N\Sigma I_{11}^{(2n)}+\left(\frac{\beta_N}{\beta_1}\right)\Sigma I_{12}^{(2n+1)}$$

$$A_-=\gamma_N^2D_-=\gamma_1\gamma_N\Sigma I_{22}^{(2n)}+\left(\frac{\gamma_N}{\gamma_1}\right)\Sigma I_{21}^{(2n+1)}$$

$$B_+=\gamma_N^2C_+=\gamma_1\gamma_N\Sigma I_{11}^{(2n)}+\left(\frac{\gamma_N}{\gamma_1}\right)\Sigma I_{12}^{(2n+1)}$$

$$B_-=\beta_N^2C_-=\beta_1\beta_N\Sigma I_{22}^{(2n)}+\left(\frac{\beta_N}{\beta_1}\right)\Sigma I_{21}^{(2n+1)}\,. \quad (30)$$

It can be shown that infinite series $\Sigma I_{ii}^{(2n)}$ and $\Sigma I_{ij}^{(2n+1)}$ converge absolutely (see Appendix). In some particular cases (§ 3 and § 4), the first term is sufficient for the crystal waves to be accounted for. In this case

$$A_+=B_-=\beta_1\beta_N,\quad A_-=B_+=\gamma_1\gamma_N$$
$$C_-=D_+=(\beta_1/\beta_N),\quad C_+=D_-=(\gamma_1/\gamma_N). \quad (31)$$

These are constant with respect to position z. Then we can retain the conception of the dispersion surface. Crystal waves can be described by an interference between two waves which belong to two branches of the dispersion surface, although the wave length changes according to crystal distortions.

In the second approximation, the skew components $I_{ij}^{(1)}$ appear in A, B, C, and D. This does mean that scattering waves are created due to crystal distortions. If we change the variable z to h through

$$(\varphi^2+B^2)^{\frac{1}{2}}dz=B\,dh$$

we can see $I_{ij}^{(1)}$ are proportional to a Fourier coefficient of lattice distortion $d\varphi/dh$ modified by a factor $(\varphi_n^2+B^2)^{-1}$ which suppresses the effect of regions where the Bragg condition is not satisfied.

(b) Combination of the two-wave theory with the column approximation

The lattice distortion to which the present theory is applicable in a strict sense seems to be very restrictive at a first sight. If, however, we combine the present theory with the following column approximation we may deal with fairly general cases of lattice distortions. The column approximation in the present theory implies the following processes of calculating wave functions. We take a column of suitable size and shape around the point at which we need to know the wave function. We apply the two-wave theory to a hypothetical crystal which is perfect in lateral directions, being almost the same as the real crystal within the column. Finally, the wave function due to the real crystal is approximated by the wave function due to this hypothetical one at the point concerned. These processes may be justified if it is possible to find a suitable column which satisfies the following conditions: (*a*) within the column an incident wave and the corresponding diffracted wave can be specified by a set of discrete values of (ξ, η) and (ξ', η') respectively and (*b*) the surrounding regions outside the column have no effect on the wave function at the central region of the column. Critical conditions for these will be discussed in § 5.

In the cases of electron problems (Heidenreich, 1949; Hashimoto, 1960; Hirsch *et al.*, 1960) the direction of columns has been taken either along the direction of the incident wave or along the diffracted wave. Actually, however, the crystal wave propagates in a direction lying between these directions (Laue, 1952, 1953; Ewald, 1958; Kato, 1952, 1958). Therefore it is more reasonable to take the direction of the column along the direction of wave propagation. In electron cases, nevertheless, it is almost unnecessary to emphasize this alteration since the Bragg angle is small enough. In X-ray cases, on the other hand, the dif-

ference between the direction of wave propagation and the directions of the incident and diffracted wave is recognizable in ordinary experimental conditions for large single crystals. Moreover, as will be seen in § 4(*b*), the direction of the wave propagation is bent due to lattice distortions. In this case it is more adequate to take a bent column in which the crystal wave propagates along the adopted column in a self-consistent manner. If lattice distortions are too large, of course, we cannot define such a column which satisfies this self-consistency and the conditions (*a*) and (*b*) altogether.

3. Intensity anomaly of (h, k, l) and $(\bar{h}, \bar{k}, \bar{l})$ reflections

In X-ray traverse topographs for Si single crystals, Lang (1958) observed first that the topograph image of distorted regions due to (h, k, l) and $(\bar{h}, \bar{k}, \bar{l})$ reflections are different in integrated intensity.* The distortion with which we are concerned here is, for example, the one which is extended over a fairly wide area due to an array of the same-signed dislocations.

We start our discussion with a non-absorbing case. The **R**-matrix can be transposed to an **R**′-matrix by a diagonal matrix **T** as

$$\mathbf{R} = \mathbf{T}\mathbf{R}'\mathbf{T}^{-1} \tag{32}$$

where

$$\mathbf{T} = \begin{pmatrix} (\zeta'/\zeta)^{\frac{1}{2}} & 0 \\ 0 & (\zeta/\zeta')^{\frac{1}{2}} \end{pmatrix} \tag{33}$$

$$\mathbf{R}' = \begin{pmatrix} \exp i\varphi\Delta z & 0 \\ 0 & \exp -i\varphi\Delta z \end{pmatrix} \begin{pmatrix} a & iB\Delta z \\ iB\Delta z & a^* \end{pmatrix} \tag{34}$$

Thus we have

$$\mathbf{K} = \mathbf{T}\mathbf{K}'\mathbf{T}^{-1} \tag{35}$$

and

$$\mathbf{K}' = \mathbf{R}'_N\mathbf{R}'_{N-1}\ldots\mathbf{R}'_1 . \tag{36}$$

In non-absorbing cases the matrices $\{\mathbf{R}'_i\}$ are unitary matrices, so that $\mathbf{K}'$ is also unitary. Thus, generally,

$$|K'_{12}| = |K'_{21}| . \tag{37}$$

From equation (I·47),

$$I_{hkl} = \frac{\zeta'}{\zeta}|K_{21}|^2 = |K'_{21}|^2$$

$$I_{\bar{h}\bar{k}\bar{l}} = \frac{\zeta}{\zeta'}|K_{12}|^2 = |K'_{12}|^2 .$$

Therefore

$$I_{hkl} = I_{\bar{h}\bar{k}\bar{l}} . \tag{38}$$

This statement holds independently of a parameter φ; consequently, the incident angle and a type of crystal distortions. We cannot expect any anomaly mentioned above.

Next we consider absorbing crystals. If the crystal distortion is small, neglecting higher terms of the series, C and D are given by equation (31). From this it follows that

$$C_+ = D_- > C_- = D_+$$

if $\varphi_N > \varphi_1$ or *vice versa*. Moreover, if B^2 is a complex quantity due to periodic distribution of absorbing centers we have

$$|\exp i\int(\varphi^2+B^2)^{\frac{1}{2}}dz| > |\exp -i\int(\varphi^2+B^2)^{\frac{1}{2}}dz|$$

assuming the imaginary part of B^2 is negative. Therefore, neglecting the oscillation term, *i.e.* the cross term of $C_\pm$ and $D_\pm$, we have

$$|K'_{12}| > |K'_{21}| \tag{39}$$

or *vice versa* depending upon the relative magnitude of φ_1 and φ_N and the sign of the imaginary part of B^2. This is true for all φ_1, namely for the whole incident angle. Thus we can expect an anomaly due to slight distortions under the presence of the Borrmann absorption.

In highly distorted crystals, we cannot neglect higher terms in $C_\pm$ and $D_\pm$, which include factors such as

$$\exp \pm 2i\int(\varphi^2+B^2)^{\frac{1}{2}}dz .$$

In this case C_- and D_- may be larger than C_+ and D_+ respectively under the condition that the imaginary part of B^2 is negative. Therefore it is rather difficult to get a general conclusion on the magnitude of $|K'_{12}|$ and $|K'_{21}|$.

Returning to the original form of matrix multiplication (see Fig. 1 and equation (12)), however, we can see that the segments on the line 1–1 and the segments on the line 2–2 are equally distributed in a statistical sense for all possible passes including many bridging segments. Therefore, roughly speaking, the abnormal increasing of matrix elements on one line (say 1–1) due to the imaginary part of B^2 might be cancelled by the abnormal attenuation of elements on the other line (say 2–2). This situation might explain disappearance of the Borrmann effects in highly distorted crystals, which is observed in dislocation images produced with X-rays (Borrmann *et al.*, 1958) as well as electrons (Whelan *et al.*, 1960) and in elastically deformed crystals (for example, Hildebrandt, 1959; Hunter, 1959; Ishii & Kohra, 1959) in X-ray cases.

4. Bending of Pendellösung fringes

(a) Electron micrographs

Pendellösung fringes in electron micrographs are called extinction contours or equal-inclination fringes in parallel-sided crystals and called equal-thickness

* Traverse patterns are produced by an integrated intensity diffracted from individual points at the exit surface (see Kato, 1961).

fringes in wedge-shaped crystals. Since both cases and more complicated cases can be treated by similar principles, we consider here extinction contours as an example. Particular attention will be drawn to contours which appear almost perpendicularly to a screw dislocation (Fig. 2(*a*)).

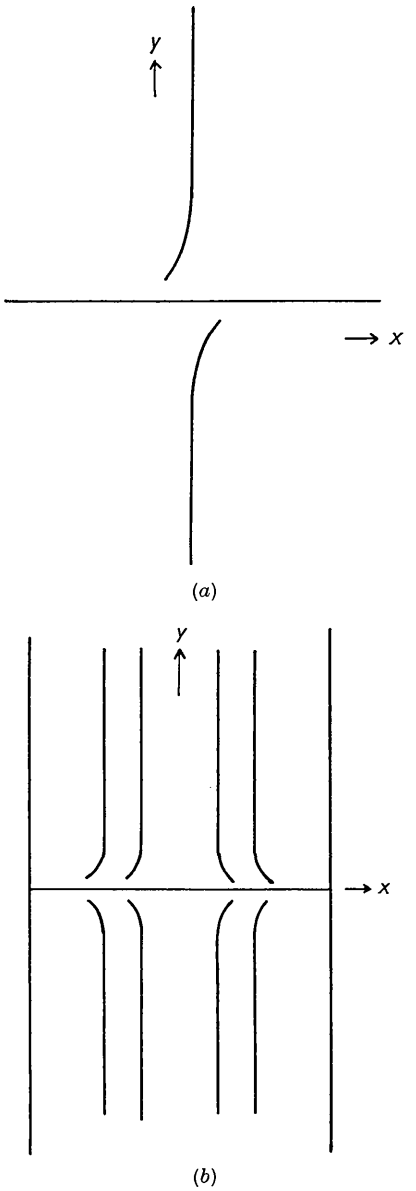

Fig. 2. Bending of extinction contours near a screw dislocation (*x*-axis). (*a*) Electron micrographs. (*b*) X-ray section topographs.

Take x and y in the direction of a dislocation line and extinction contours respectively and the origin at a point on the central line of the dislocation. Using the approximation (31), contours are given by an interference condition through equations (28) and (29)

$$2\int_{z_1}^{z_N}(\varphi^2+B^2)^{\frac{1}{2}}dz=\text{const.} \tag{40}$$

In our present problem we can write

$$\varphi=\varphi_0(x)+\Delta\varphi(y,z)\,. \tag{41}$$

The term $\varphi_0(x)$ expresses lattice bending extended over the whole crystal and $\Delta\varphi$ expresses local distortions due to the dislocation. Obviously $\Delta\varphi$ tends to zero with increasing $|y|$. We take a contour line which satisfies the condition (40) for a particular φ_0 at a large $|y|$. Near the dislocation $\Delta\varphi$ takes an appreciable value, so that the same value of φ_0 no longer satisfies the same condition. Thus we can expect a bending of the contour.

It follows immediately from the condition (40) that if a pair $(\varphi_0, \Delta\varphi)$ satisfies the condition another pair $(-\varphi_0, -\Delta\varphi)$ satisfies the same condition. On the other hand the elasticity theory of dislocations tells us that $\Delta\varphi(y,z)=-\Delta\varphi(-y,z)$ (Koehler, 1941). Also, in a simple case of homogeneous bending of the crystal, $\varphi_0(x)=-\varphi_0(-x)$ taking the origin as $\varphi_0(0)=0$. Thus we can expect that contours must have a symmetry of inversion with respect to the origin. Results are qualitatively in accordance with experiments (Menter, 1960; Kamiya & Uyeda, 1961).

(*b*) *X-ray topographs*

In this section we are concerned with section patterns of X-ray diffraction topographs. As discussed in previous papers (Kato, 1961*a*, *b*), section patterns are fully understood only in terms of a spherical wave theory. The theory is derived from a plane-wave theory as described in the last paragraph of § 3(*a*) of part I (Kato, 1963). In the present case, $\binom{K_{11}}{K_{21}}$ of equation (I·47) should be given by equations (28) and (29) of this paper and $N\Phi$ must be replaced by $\Sigma\Phi_n$ where Φ_n is defined by equation (6). Thus the wave fields at the exit surface due to diffraction waves are given by

$$\begin{aligned} f_a^g=\int_{-\infty}^{+\infty}&\exp i\left[\delta t_0\varphi_0-\int_{z_1}^{z_N}\varphi\,dz\right]\\ &\times\left\{\tilde{D}_+\exp i\int_{z_1}^{z_N}(\varphi^2+B^2)^{\frac{1}{2}}dz\right.\\ &\left.+\tilde{D}_-\exp -i\int_{z_1}^{z_N}(\varphi^2+B^2)^{\frac{1}{2}}dz\right\}d\varphi_0 \end{aligned} \tag{42}$$

where t_0 is the thickness of the crystal and δ is a constant, proportional to the length of a perpendicular from an observation point to the direction of the incident wave which satisfies the Bragg condition exactly.* $\tilde{D}_+$ and $\tilde{D}_-$ are amplitudes which are constant with respect to z under the approximation of equation (31).

* Exactly, $(1-\delta)$ is q/α in the notation used in the previous papers (Kato, 1961).

In order to calculate f_a^g, we use an approximation of stationary phase (for example, Jeffreys & Jeffreys, 1946). Wave fields f_a^g are proportional to the integrand itself of equation (42) in which φ_0 is replaced by φ_+ for $\tilde{D}_+$-wave and φ_- for $\tilde{D}_-$-wave respectively. Here φ_+ and φ_- are φ_0-values at stationary points of the phase with respect to φ_0, so that they are given by

$$(1-\delta)t_0 = f(\varphi_+) \tag{43}$$

and

$$(1-\delta)t_0 = -f(\varphi_-)$$

where

$$f(\varphi_0) = \int_{z_1}^{z_N} (\varphi_0 + \Delta\varphi)/\{(\varphi_0+\Delta\varphi)^2 + B^2\}^{\frac{1}{2}} dz\,. \tag{44}$$

In general φ_+ is not equal to $-\varphi_-$ so that Pendellösung interference does not occur between conjugate waves as does in perfect crystals. This means that crystal waves do not propagate in a straight direction in a distorted crystal.

Fringe contours are given by a condition for phase difference between $\tilde{D}_+$ and $\tilde{D}_-$ wave, namely

$$\left[\int_{z_1}^{z_N} \{(\varphi_+ + \Delta\varphi)^2 + B^2\}^{\frac{1}{2}} dz + \delta t_0 \varphi_+ - \int_{z_1}^{z_N} (\varphi_+ + \Delta\varphi) dz\right] - \left[-\int_{z_1}^{z_N} \{(\varphi_- + \Delta\varphi)^2 + B^2\}^{\frac{1}{2}} dz + \delta t_0 \varphi_- - \int_{z_1}^{z_N} (\varphi_- + \Delta\varphi) dz\right] = \text{const.} \tag{45}$$

This indicates that bending of Pendellösung fringes should be expected also in X-ray cases.

The saddle points φ'_+ and φ'_- of $\tilde{D}_+$- and $\tilde{D}_-$-waves for a reverse distortion $-\Delta\varphi$ are given in a similar way

$$(1-\delta)t_0 = g(\varphi'_+) \tag{46}$$

and

$$(1-\delta)t_0 = -g(\varphi'_-)$$

where

$$g(\varphi_0) = \int_{z_1}^{z_N} (\varphi_0 - \Delta\varphi)/\{(\varphi_0-\Delta\varphi)^2 + B^2\}^{\frac{1}{2}} dz\,. \tag{47}$$

Fringe contours are also given by an equation similar to equation (45), in which the set of quantities $(\varphi_+, \varphi_-, \Delta\varphi)$ are replaced by another set of $(\varphi'_+, \varphi'_-, -\Delta\varphi)$.

Comparing equations (43) and (44) with (46) and (47) we have

$$\varphi_+ = -\varphi'_- \quad \text{and} \quad \varphi_- = -\varphi'_+\,. \tag{48}$$

Thus we can see that if a pair (φ_+, φ_-) satisfies the phase condition (45) for a distortion $\Delta\varphi$, another pair (φ'_+, φ'_-) satisfies the same condition for the reverse distortion $-\Delta\varphi$.

We consider again a simple case where a screw dislocation lies in a parallel-sided crystal perpendicularly to the net plane concerned. An observation point on the exit surface is specified by x and y coordinates as shown in Fig. 2(*b*). If no distortion is present, we have parallel fringes along y direction (Kato, 1961*a*, *b*). Since δ is only a function of x on the present choice of axes, $\varphi_\pm$ and $\varphi'_\pm$ are functions of x directly and functions of y through a functional form of $\Delta\varphi$. As described above, $\Delta\varphi(y,z) = -\Delta\varphi(-y,z)$. Therefore two sets $(\varphi_+, \varphi_-, \Delta\varphi)$ and $(\varphi'_+, \varphi'_-, -\Delta\varphi)$ corresponding to the observation points (x, y) and $(x, -y)$ satisfy the same phase condition (45). In other words, fringe patterns around a dislocation must have mirror-symmetry with respect to the dislocation line (see Fig. 2(*b*)). Some observations by Lang are in accordance with this conclusion (Lang, 1959). It is interesting to notice the contrast between electrons and X-rays.

5. Applicability of the two-wave theory combined with the column approximation

As described in § 2(*b*) two conditions are to be satisfied for applying the present theory to real crystals. We consider these conditions in a semi-quantitative way. Here we consider only the critical conditions with respect to the variation of lattice in the plane including the incident wave and the diffracted wave, assuming perfectness in the direction perpendicular to this plane. So that the problem is reduced to a two-dimensional one. The change of lattice along the direction perpendicular to the plane concerned can be treated in a similar way.

Let us consider a crystal slice and limit the lateral size by a diaphragm* of width S on it. If a plane wave impinges the reflected wave has a line width Ω due to lattice distortions and also due to limiting the crystal size. Increasing the width S, Ω may be approximated by $2\pi(\Delta g/K)$, where Δg is the width of distribution of local $\mathbf{g}$-vector in a direction perpendicular to the reflected beam within the column limited by the aperture S. Decreasing the width S, Δg may tend to zero. In this case, however, Ω should be approximated by λ/S, in which λ is the wave length, because diffraction due to the crystal size becomes predominant. Thus, we have an intrinsic line broadening Ω_m, which may be estimated by an intersection of the above-mentioned two curves of Ω versus S. As the results the intrinsic variations in g_1 and g_2 as well as in φ are unavoidable in the column. The last is given by $\Delta\varphi_m = \frac{1}{2}\Omega_m(\xi'^2+\eta'^2)^{\frac{1}{2}}$, through equations (I·17) and (I·29). The critical condition (*a*), therefore, may be given by

$$\varphi_m \ll B\,. \tag{49}$$

Since an angular width $\Delta\theta$ of the Bragg reflection is given by $2B/(\xi^2+\eta^2)^{\frac{1}{2}}$ equation (49) is also read as

$$\Omega_m \ll \Delta\theta\left(\frac{\xi^2+\eta^2}{\xi'^2+\eta'^2}\right)^{\frac{1}{2}} \sim \Delta\theta\,. \tag{49'}$$

* The word 'slit' would be better than 'diaphragm'. However, the latter is preferred here in order to accord with the usage in a previous paper (Kato, 1952).

As described in § 2(*b*), the direction of the column should be a direction of wave propagation in general cases. Using W for the angular width of wave propagation corresponding to the angular width Ω of the wave vector the sufficient condition for (*b*) is given by

$$W(\Omega_m)t_e \ll S_m \tag{50}$$

where t_e is an effective thickness of the region where the crystal is appreciably distorted.

As a simple example we consider a lattice distortion due to an edge dislocation lying in the y-direction with the slip plane in the xy-plane. The net plane is assumed to be the yz-plane. Displacements (u, v, w) are given by Koehler (1941). A gradient $(\partial u/\partial z)$ corresponds to the inclination of the net plane. The width, Ω, of this inclination over the crystal of width S in the vicinity of a point $x=D$ is approximately

$$\Omega = S\{\partial^2 u/\partial x \partial z\}_{x=D,\, z=0}\,.$$

The width Ω_m and S_m are given by this equation and $\Omega = \lambda/S$, so that

$$\begin{aligned}\Omega_m &= \sqrt{(\lambda\tau)/D}\\ S_m &= \sqrt{(\lambda/\tau)D}\end{aligned}$$

where τ is $(b/4\pi)(3-2\nu)/(1-\nu)$, b and ν being the magnitude of Burger's vector and Poisson's ratio respectively.

Numerically, τ is of the order of 10^{-8} cm. for usual substances. Inserting reasonable figures, $\lambda = 5\times10^{-2}$ Å, $\Delta\theta \sim 10^{-2}$ for electrons and $\lambda = 1$ Å, $\Delta\theta \sim 10^{-5}$ for X-rays, the condition (49′) gives

$$\begin{aligned}&D > 22 \text{ Å} \quad &&\text{(for electrons)}\\ &D > 10\,\mu &&\text{(for X-rays)}\,.\end{aligned} \tag{51}$$

The second condition for the column approximation is through equation (50) that

$$t_e < \alpha D^2/\tau \tag{52}$$

where α is a numerical factor corresponding to the ratio of Ω_m and W. This is larger than 10^{-1} for electrons whereas larger than 10^{-4} for X-rays (see equation (36) of Kato, 1961*a*). Since $t_e \simeq D$ in dislocation cases, (52) is satisfied if

$$\begin{aligned}&D > 10 \text{ Å} \quad &&\text{(for electrons)}\\ &D > 1\,\mu &&\text{(for X-rays)}.\end{aligned}$$

Thus in this example we can see that the first condition is more severe than the second. Following these arguments, it is concluded that the present theory is applicable to most practical cases of electrons. On the other hand, in X-ray cases, the theory is applicable only to a region more than 10μ outside a dislocation core.

In fact, in X-ray section topographs, central regions of 20μ in diameter have entirely different characters compared with the outer region in which Pendellösung fringes appear as slightly bent. In the core region Pendellösung fringes disappear.

APPENDIX

A. *Matrix elements of* $I_{ij}^{(2n)}$ *and* $I_{ij}^{(2n+1)}$.

Inserting equation (20) into equation (18) we have

$$\begin{aligned}H_{12}^{(1)} &= H_{11}^{(0)}(B^2/2\beta_1^2)\int_{z_1}^{z_N} P_-(t)\,dt\\ H_{21}^{(1)} &= H_{22}^{(0)}(B^2/2\gamma_1^2)\int_{z_1}^{z_N} P_+(t)\,dt\end{aligned} \tag{A1}$$

where

$$P_\pm = \left\{\left(\frac{d\varphi}{dz}\right)\Big/(\varphi^2+B^2)\right\}_{z=t} \exp\,\pm 2i\int_{z_1}^{t}(\varphi^2+B^2)^{\frac{1}{2}}dz\,. \tag{A2}$$

In a similar way we can easily obtain

$$\begin{aligned}H_{11}^{(2)} &= H_{11}^{(0)}\left(\frac{i}{2}B\right)^2\int_{r>s}\int Q_-(r,s)\,dr\,ds\\ H_{22}^{(2)} &= H_{22}^{(0)}\left(\frac{i}{2}B\right)^2\int_{r>s}\int Q_+(r,s)\,dr\,ds\end{aligned} \tag{A3}$$

where

$$\begin{aligned}Q_\pm = \left\{\left(\frac{d\varphi}{dz}\right)\Big/(\varphi^2+B^2)\right\}_{z=r}&\left\{\left(\frac{d\varphi}{dz}\right)\Big/(\varphi^2+B^2)\right\}_{z=s}\\ &\times\exp\,\pm 2i\int_r^s(\varphi^2+B^2)^{\frac{1}{2}}dz\,.\end{aligned} \tag{A4}$$

From Fig. 1, we can see that the integrand of $H_{ii}^{(2n)}$ and $H_{ij}^{(2n+1)}$ can be expressed in terms of $P_\pm$ and $Q_\pm$. Thus we can write them down easily. From these $I_{ii}^{(2n)}$ and $I_{ij}^{(2n+1)}$, defined by equations (24) and (25), are given as follows:

$$\begin{aligned}I_{11}^{(2n)} &= \left(\frac{B}{2}i\right)^{2n}\int_{r_n>s_n>\cdots>r_1>s_1}\cdots\cdots\int\prod_{i=1}^{n}Q_-(r_i,s_i)\,dr_i\,ds_i\\ I_{22}^{(2n)} &= \left(\frac{B}{2}i\right)^{2n}\int_{r_n>s_n>\cdots>r_1>s_1}\cdots\cdots\int\prod_{i=1}^{n}Q_+(r_i,s_i)\,dr_i\,ds_i\end{aligned} \tag{A5}$$

$$\begin{aligned}I_{12}^{(2n+1)} &= \left(\frac{B^2}{2}\right)\left(\frac{B}{2}i\right)^{2n}\\ &\times\int_{r_n>s_n>\cdots>r_1>s_1>t}\cdots\cdots\int\prod_{i=1}^{n}Q_-(r_i,s_i)P_-(t)\,dr_i\,ds_i\,dt\\ I_{21}^{(2n+1)} &= \left(\frac{B^2}{2}\right)\left(\frac{B}{2}i\right)^{2n}\\ &\times\int_{r_n>s_n>\cdots>r_1>s_1>t}\cdots\cdots\int\prod_{i=1}^{n}Q_+(r_i,s_i)P_+(t)\,dr_i\,ds_i\,dt\end{aligned} \tag{A6}$$

B. *Convergency of* $\Sigma I_{ii}^{(2n)}$ *and* $\Sigma I_{ij}^{(2n+1)}$

First we consider $|I_{11}^{(2n)}| = |I_{22}^{(2n)}|$.

$$\begin{aligned}|I_{11}^{(2n)}| &\le \left(\frac{B}{2}\right)^{2n}\int_{r_n>s_n}\cdots\int\prod_{i=1}^{n}|Q_\pm(r_i,s_i)|\,dr_i\,ds_i\\ &= \left(\frac{B}{2}\right)^{2n}\int_{r_n>s_n}\cdots\int\prod_{i=1}^{n}\left\{\left|\frac{d\varphi}{dz}\right|\Big/(\varphi^2+B^2)\right\}_{r_i}\\ &\qquad\times\left\{\left|\frac{d\varphi}{dz}\right|\Big/(\varphi^2+B^2)\right\}_{s_i}dr_i\,ds_i\\ &= \left(\frac{B}{2}\right)^{2n}\frac{1}{(2n)!}\left\{\int_{z_1}^{z_N}\left|\frac{d\varphi}{dz}\right|\Big/(\varphi^2+B^2)\,.\,dz\right\}^{2n}.\end{aligned} \tag{B1}$$

On the other hand

$$\int_{z_1}^{z_N} \left|\frac{d\varphi}{dz}\right| \Big/ (\varphi^2+B^2).dz \leq (m+1)\int_{-\infty}^{+\infty} \frac{d\varphi}{\varphi^2+B^2} = \frac{\pi}{B}(m+1) \qquad \text{(B2)}$$

where m is the number of maxima and minima of $d\varphi/dz$ between z_N and z_1. Thus, it follows that

$$|I_{11}^{(2n)}| \leq \frac{1}{(2n)!}\{(m+1)\tfrac{1}{2}\pi\}^{2n}. \qquad \text{(B3)}$$

In a similar way

$$|I_{11}^{(2n+1)}| \leq \frac{1}{(2n+1)!}\{(m+1)\tfrac{1}{2}\pi\}^{2n+1}. \qquad \text{(B4)}$$

Therefore we can see $\Sigma I_{ij}^{(2n)}$ and $\Sigma I_{ij}^{(2n+1)}$ converge absolutely.

The author would like to express his sincere thanks to Dr A. R. Lang for his valuable discussion and kind encouragement throughout this work. He also wishes to express his thanks to Dr J. W. Menter, Dr P. B. Hirsch, Dr M. J. Whelan and Dr A. Howie who kindly gave him opportunities of seeing their interesting electron micrographs.

References

Borrmann, G., Hartwig, W. & Irmler, H. (1958). *Z. Naturforsch.* **139**, 423.
Ewald, P. P. (1958). *Acta Cryst.* **11**, 888.
Hashimoto, H. & Mannami, M. (1960). *Acta Cryst.* **13**. 363.
Hashimoto, H. Howie, A. & Whelan, J. M. (1960). *Phil. Mag.* **5**, 967.
Heidenreich, R. D. (1949). *J. Appl. Phys.* **20**, 993.
Hildebrandt, G. (1959). *Z. Kristallogr.* **112**, 312.
Hirsch, P. B., Horne, R. W. & Whelan, M. J. (1956). *Phil. Mag.* **1**, 677.
Hirsch, P. B., Howie, A. & Whelan, M. J. (1960). *Phil. Trans. Roy. Soc. Lond.* **252**, 499.
Howie, A. & Whelan, M. J. (1961). *Proc. Roy. Soc.* A, **263**, 217.
Hunter, L. P. (1959). *J. Appl. Phys.* **30**, 874.
Ishii, Z. & Kohra, K. (1959). *J. Phys. Soc. Japan*, **14**, 1250.
Kamiya, Y. & Uyeda, R. (1961). *J. Phys. Soc. Japan.* **16**, 1361.
Kato, N. (1952). *J. Phys. Soc. Japan*, **7**, 397.
Kato, N. (1958). *Acta Cryst.* **11**, 885.
Kato, N. (1961*a*). *Acta Cryst.* **14**, 526.
Kato, N. (1961*b*). *Acta Cryst.* **14**, 627.
Kato, N. (1963). *Acta Cryst.* **16**, 276.
Koehler, J. S. (1941). *Phys. Rev.* **60**, 397.
Lang, A. R. (1958). *J. Appl. Phys.* **29**, 597.
Lang, A. R. (1959*a*). *J. Appl. Phys.* **30**, 1748.
Lang, A. R. (1959*b*). Private communication.
Laue, M. v. (1952). *Acta Cryst.* **5**, 619.
Laue, M. v. (1953). *Acta Cryst.* **6**, 217.
Menter, J. W. (1960). Private communication.
Newkirk, J. B. (1958). *Phys. Rev.* **110**, 1465.
Warren, B. E. & Averbach, B. L. (1950). *J. Appl. Phys.* **21**, 595.
Wilson. A. J. C. (1952). *Acta Cryst.* **5**, 318.

Acta Cryst. (1963). **16**, 290

Electron Diffraction Study on Thin Films of Polymers of *p*-Halogeno-styrene

By Kinya Katada*

Faculty of Science, Osaka City University, 12 *Minami-ogimachi, Kita-ku, Osaka, Japan*

(*Received* 23 *October* 1961 *and in revised form* 7 *March* 1962)

Thin films of polymers of *p*-Cl-, *p*-Br- and *p*-I-styrene obtained by radical polymerization were studied by electron diffraction. Ten to thirteen halos were obtained by using a sector-camera. Intensity curves for some assumed models were calculated and were compared with the observed ones. In the cases of the Br- and I-derivatives the complex atomic scattering factors were used for the calculation. The radial distribution method was applied to the Cl-derivative.

The following results are common to all three kinds of halogen derivatives. A linear molecule is built up of styrene residues connected in a 'head to tail' arrangement, and their benzene rings are located alternately on each side of the plane of the zig-zag paraffin chain. Neighboring molecules are closely packed in a 'face to face' configuration in a plane perpendicular to the chain. These regularities in the structure are maintained only among the nearest neighbor residues.

1. Introduction

Several electron diffraction studies of amorphous thin films have been reported. Since more halos can be obtained by electron diffraction than by X-ray diffraction, the former method is better suited to a structure analysis of the shorter interatomic distances. There have been few studies, however, in which this usefulness of electron diffraction has been exploited. In the present study, this merit of electron diffraction

* Present address: Faculty of Science, Osaka City University, Sugimotocho, Sumiyoshi-ku. Osaka, Japan.